УДК 629.12.03
Р93

DEVELOPMENT OF SHIP SYSTEMS FOR AIR PURIFICATION FROM DROPLET MOISTURE

РАЗРАБОТКА СУДОВЫХ СИСТЕМ ОЧИСТКИ ВОЗДУХА ОТ КАПЕЛЬНОЙ ВЛАГИ

DOI 10.15589/SMI20170220

Serhiy S. Ryzhkov
Рыжков Сергей Сергеевич

Serhiy S. Ryzhkov С. С. Рижков, канд. техн. наук, доц.
sergiy.ryzhkov@nuos.edu.ua
ORC ID: 0000-0002-2201-6172

Admiral Makarov National University of Shipbuilding, Nikolaev
Национальный университет кораблестроения имени адмирала Макарова, г. Николаев

Abstract. The study of gas dynamics and deposition coefficients of the separating profile has been performed. The three-dimensional model of working channels of the ship systems for air purification from droplet moisture is developed. The distribution of velocity, static pressure, dynamic pressure, kinetic energy of turbulence, and deposition coefficients for the flow rates of 5, 10, 15, 20 m/s in separating profiles with the radii of 5, 10, 15, 20, 25 mm. The droplet moisture deposition coefficient is 99.9 %. Designs of the ship systems for air purification from droplet moisture are developed for the air flow ranging from 20 to 2000 m^3/hour.

Keywords: separator; air purification system; moisture separator; 3D modeling.

Аннотация. Выполнены исследования газодинамики и коэффициентов осаждения сепарационного профиля. Разработаны трехмерные модели рабочих каналов судовых систем очистки воздуха от капельной влаги. Получено распределение скорости, статического давления, динамического давления, кинетической энергии турбулентности и коэффициентов осаждения для скоростей потока 5, 10, 15, 20 м/с в сепарирующих профилях с радиусами 5, 10, 15, 20, 25 мм. Разработаны конструктивные решения судовых систем очистки воздуха от капельной влаги для расхода воздуха от 20 до 2000 $м^3$/ч.

Ключевые слова: сепаратор; системы очистки воздуха; влагоотделитель; 3D-моделирование.

Анотація. Виконано дослідження газодинаміки та коефіцієнтів осадження сепараційного профілю. Розроблено тривимірні моделі робочих каналів судових систем очищення повітря від краплинної вологи. Отримано розподіл швидкості, статичного тиску, динамічного тиску, кінетичної енергії турбулентності та коефіцієнтів осадження для швидкостей потоку 5, 10, 15, 20 м/с у сепаруючих профілях з радіусами 5, 10, 15, 20, 25 мм. Розроблено конструктивні рішення суднових систем очищення повітря від краплинної вологи для витрат повітря від 20 до 2000 $м^3$/год.

Ключові слова: сепаратор; системи очищення повітря; вологовіддільник; 3D-моделювання.

References

[1] Belousov V. V. *Teoreticheskiye osnovy protsessov gazoochistki* [Theoretical foundations of gas purification processes]. Moscow, Metallurgiya Publ., 1988. 256 p.

[2] Ryzhkov S. S., Basok B. I. *Ekologicheskiye resursosberegayushchiye tekhnologii dlya promyshlennoy teplotekhniki na osnove dispersnykh dvukhfaznykh sred* [Ecological resource-saving technologies for industrial heat engineering based on dispersed two-phase media]. *Promyshlennaya teplotekhnika — Industrial heat engineering*, 2001, no. 4–5, pp. 141 – 145.

[3] Van-Dayka M. *Techeniye zhidkosti i gaza* [Liquid and gas flow]. Moscow, Mir Publ., 1986. 114 p.

[4] Rayst P. *Aerozoli. Vvedeniye v teoriyu* [Aerosols. Introduction to the theory]. Moscow, Mir Publ., 1987, pp. 34-40.

[5] Mednikov Ye. P. *Turbulentnyy perenos i osazhdeniye aerozoley* [Turbulent transfer and deposition of aerosols]. Moscow, Nauka Publ., 1981. 176 p.

[6] Kalvert S., Inglund G. M. *Zashchita atmosfery ot promyshlennykh zagryazneniy: Spravochnik Ch. 1* [Protection of the atmosphere from industrial pollution: Handbook. Part 1]. Moscow, Metallurgiya Publ., 1988. 760 p.

[7] Ryzhkov S. S., Kharytonov Yu. M., Blahodatnyi V. V. *Metody ochyshchennia povitrianoho seredovyshcha vid zabrudnen* [Methods for the air medium purification from contaminants]. Mykolaiv, UDMTU Publ., 2002. 56 p.

Problem statement. Providing comfort in ship accommodations and service premises, as well as maintaining necessary technological conditions in production premises, requires air purification from droplet moisture. Moisture ingress into the air duct leads to the dampness of air-conditioned rooms, intense corrosion of equipment, which can lead to accumulation of moisture in certain areas, etc. It is reasonable to increase the efficiency and reduce the dimensions of ship systems intended for air purification from droplet moisture through designing devices with the most effective deposition surfaces with the help of separation gradient aerosol technologies. The development of models and research methods that allow for the calculation of gas dynamics in the working channels of the purification systems and deposition coefficients for the equipment's entire operating range will provide the basis for the development of ship systems for air purification from droplet moisture.

Latest research and publication analysis. At present, vast use is made of inertial separators, the separating elements of which either have demister pads or are empty and provide internal drainage of droplet moisture [1]. Tests of the mist eliminators described in [2] have showed their insufficient separation ability and increased aerodynamic drag. In addition, the manufacture of such separating elements requires a large amount of work that can not be mechanized. A possible solution is the development of high-efficiency gradient separators of aerosol media for ship power plants. Creation of the technologies for separation of aerosol media with the use of new phase capture techniques offers a significant reserve for energy saving. It is promising to develop innovative methods implementing gradient intensification of the transfer processes in the boundary layers of multifunctional surfaces of power plants. The multifunctional surfaces include those characterized with a compactness coefficient exceeding 2000 m^2/m^3, enhanced heat exchange, and separating properties. The use of methods and techniques for designing and implementing filters based on gradient technologies will increase the reliability and service life of the ship's power equipment and its elements. In turn, this will promote the creation of high-efficiency energy-saving technologies and efficient design solutions for a wide range of gradient separators of ship power plants [5].

THE ARTICLE AIM is to present the development of ship systems for air purification from droplet moisture.

The aim can be achieved by tackling the following objectives:

– to perform mathematical modeling of the processes at the initial velocities of 5, 10, 15, 20 m/s on the basis of separation gradient aerosol technologies at different flow rates in the separating profiles with the radii of 5, 10, 15, 20, 25 mm;

– to calculate the distribution of velocity, static pressure, dynamic pressure, kinetic energy of turbulence, and deposition coefficients on the basis of separation gradient aerosol technologies for the flow rates of 5, 10, 15, 20 m/s in separating profiles with the radii of 5, 10, 15, 20, 25 mm;

– to calculate the coefficient of deposition of droplet moisture for the flow rates of 5, 10, 15, 20 m/s in separating profiles with the radii of 5, 10, 15, 20, 25 mm;

– to develop design solutions of ship systems for air purification from droplet moisture for air consumption ranging from 20 to 2000 m3/h;

– to develop and approve drawings for a lineup of ship systems for air purification from droplet moisture;

– to develop and approve the enterprise standard for the lineup of ship systems for air purification from droplet moisture.

Basic material. Mathematical modeling. The Reynolds stress transport equations $\rho\overline{u_i'u_j'}$ can be written in the following form:

$$\frac{\partial}{\partial t}\left(\rho\overline{u_i'u_j'}\right)+C_{ij}=D_{T,ij}+D_{L,ij}+P_{ij}+G_{ij}+$$
$$+\phi_{ij}-\varepsilon_{ij}+F_{ij}+S_{user}, \qquad (1)$$

where $\frac{\partial}{\partial t}\left(\rho\overline{u_i'u_j'}\right)$ is the partial derivative of time; $\tilde{N}_{ij}\equiv\frac{\partial}{\partial x_k}\left(\rho u_k\overline{u_i'u_j'}\right)$ is the convective component; $D_{T,ij}\equiv-\frac{\partial}{\partial x_k}\left[\rho\overline{u_i'u_j'u_k'}+\overline{p\left(\delta_{kj}u_i'+\delta_{ik}u_j'\right)}\right]$ represents the turbulent diffusion; $D_{L,ij}\equiv-\frac{\partial}{\partial x_k}\left[\mu\frac{\partial}{\partial x_k}\left(\overline{u_i'u_j'}\right)\right]$ is the laminar diffusion; $P_{ij}\equiv-\rho\left(\overline{u_i'u_k'}\frac{\partial u_j}{\partial x_k}+\overline{u_j'u_k'}\frac{\partial u_j}{\partial x_k}\right)$ stands for the formation of tension; $G_{ij}\equiv-\rho\beta\left(g_i\overline{u_j'\theta}+g_j\overline{u_i'\theta}\right)$ is the formation of buoyancy force; $\phi_{ij}\equiv p\left(\frac{\partial u_i'}{\partial x_j}+\frac{\partial u_j'}{\partial x_i}\right)$ indicates the stress exerted by pressure; $\varepsilon_{ij}\equiv 2\mu\overline{\frac{\partial u_i'}{\partial x_k}\frac{\partial u_j'}{\partial x_k}}$ stands for dissipation; $F_{ij}\equiv-2\rho\Omega_k\left(\overline{u_j'u_m'}\varepsilon_{ikm}+\overline{u_i'u_m'}\varepsilon_{jkm}\right)$ represents the formation of the rotational system; S_{user} is the element set by the user.

The energy equation obtained on the basis of this theory has the following form:

$$\frac{\partial}{\partial t}(\rho E)+\frac{\partial}{\partial x_i}\left[u_i(\rho E+p)\right]=$$
$$=\frac{\partial}{\partial x_j}\left[\left(k+\frac{c_p\mu_t}{\Pr_t}\right)\frac{\partial T}{\partial x_j}+u_i\left(\tau_{ij}\right)_{eff}\right], \qquad (2)$$

where E is the total energy;

$\left(\tau_{ij}\right)_{eff}=\mu_{eff}\left(\frac{\partial u_j}{\partial x_i}+\frac{\partial u_i}{\partial x_j}\right)-\frac{2}{3}\mu_{eff}\frac{\partial u_k}{\partial x_k}\delta_{ij}$ is the deviator stress tensor.

The turbulent mass transfer equation is modeled by substituting the enthalpy of equation (2) with the concentration of particles of a dispersed multiphase flow:

$$\frac{\partial}{\partial t}(\rho C)+\frac{\partial}{\partial x_i}\left[u_i(\rho C)\right]=$$
$$=\frac{\partial}{\partial x_j}\left[\left(D+\frac{\mu_t}{\rho \Pr_{tD}}\right)\frac{\partial C}{\partial x_j}+u_i\left(\tau_{ij}\right)_{eff}\right]. \qquad (3)$$

The continuity equation for the flow without the particle source at a constant density of the liquid is as follows:

$$\frac{\partial u_i}{\partial x_i}=0. \qquad (4)$$

The equation of the dynamics of the particles movement in the gas flow is written as follows:

$$\frac{\partial u_p}{\partial x_t}=F_1+F_2+F_3+F_4+F_D, \qquad (5)$$

where x_t is the time, force per unit mass of the particle; $F_1=\frac{1}{2}\frac{\rho}{\rho_k}\frac{\partial}{\partial t}(u-u_k)$ istheforceofinertia, $F_2=-0{,}5m_k\frac{\partial u_k'^2}{\partial y}$ is the force of turbophoresis, $F_3=\left(\frac{P}{P_w}\right)u_k\frac{\partial u}{\partial x}$ is the diffusiophoretic force, $F_4=\frac{2K\upsilon^{1/2}\rho d_{ij}}{\rho_p d_p\left(d_{lk}d_{kl}\right)}(\upsilon-\upsilon_P)$ is the Saffman lift force, and $\overline{F}_D=\frac{18\mu}{\rho_P d_P^2}\frac{C_D}{24}\mathrm{Re}$ is the force of resistance. In these expressions, P_w is the value of pressure of the wall, p is the flow pressure, d_P is the particle diameter, ρ_P is the particle density, υ_P is the particle velocity, ρ is the density of multiphase high-pressure fuel mixtures, υ is the gas velocity, d_{ij} is the deformation tensor, K is equal to 2.594, $\mathrm{Re}=\rho d_P\frac{|u_P-u|}{\mu}$ is the Reynolds number, u is the initial flow rate; u_P is the particle velocity; μ is the molecular viscosity of the flow; ρ is the flow density; ρ_P is the particle density; d_P is the particle diameter. The coefficient of resistance is calculated as follows:

$$C_D=\frac{24}{\mathrm{Re}}\left(1+b_1\mathrm{Re}^{b_2}\right)+\frac{b_3\mathrm{Re}}{b_4+\mathrm{Re}}, \qquad (6)$$

where b is the polynomial coefficient to be set.

The quantities C_{ij}, $D_{L,ij}$, P_{ij} and F_{ij} are calculated directly from the above expressions, while $D_{T,ij}$, G_{ij}, ϕ_{ij}, ε_{ij} are modeled in the form that allows closing the system of equations. The methods used in their modeling have been detailed in previous publications.

Upon the solution of the equations, the purification intensity is determined by the mass, hydrodynamic, and energy coefficients for intensification of deposition (labeled as *Km*, *Kh*, and *Ke*, respectively). The principles of calculation of these coefficients suggest maximizing the mass of deposited particles while minimizing the geometric volume of the processes and the mechanical work of the particles transfer relative to the internal and external energy expenditure. Based on these principles, the integrated indicator of the purification intensity *IPI* is calculated with the use of the following formula:

$$IPI = 1-(1-Km)(1-Kh)(1-Ke), \qquad (7)$$

where

$$Km = (\Sigma Miin-\Sigma Miout)/\Sigma Miin, \qquad (8)$$
$$Kh = (\Sigma Vi-\Sigma Viu)/\Sigma Vi, \qquad (9)$$
$$Ke = 1-(A+L)/(E_{int}+E_{ex}), \qquad (10)$$

In these formulas, Σ*Miin* and Σ*Miout* are the total mass of the particles with the size of *i* at the inlet and outlet of the zone, respectively; Σ*Vi* and Σ*Viu* is the total volume undergoing purification or left unprocessed, respectively; $A = \Sigma lF$ is the total work on the particles transfer over the distance l under the impact of the forces F; $L = G[\Delta(pv)+\Delta(w^2/2)+g\Delta h]+L_t+L_f$ is the work performed by the flow of the G consumption; $E_{int}=\Delta(c_v tG\tau)$ is the internal energy expenditure of the flow, while E_{ex} is the external energy expenditure.

Research results. Development of ship systems intended for air purification from droplet moisture involved a study of the separating profile (Fig. 1) with the following parameters: $R1 = (0.05\div0.5)L$; $h = (0.5\div5.0)R1$; $R2 = (0.01\div1.0)L$.

The profile under study is 80 mm long, with 2 drain grooves on the top and 2 drain grooves on the bottom; the grooves are 3 mm long and 2 mm deep. The curvature radii of the profile selected for analysis are 5, 10, 15, 20, and 25. The study of the separating profiles has been performed with the help of three-dimensional design grids (Fig. 2).

On the basis of the mathematical model of the processes, the initial and boundary conditions were set for substitution to the system of equations. It allowed calculating the basic parameters of the separating profile. For the calculation accuracy, the criterion of coincidence 10^{-4} was applied to the variables of velocity, flow continuity, kinetic energy of turbulence, and Reynolds stresses.

In the process of calculation, the following parameters were set:

- three-dimensional real-size geometry (length of 80 mm and height of 5...25 mm);

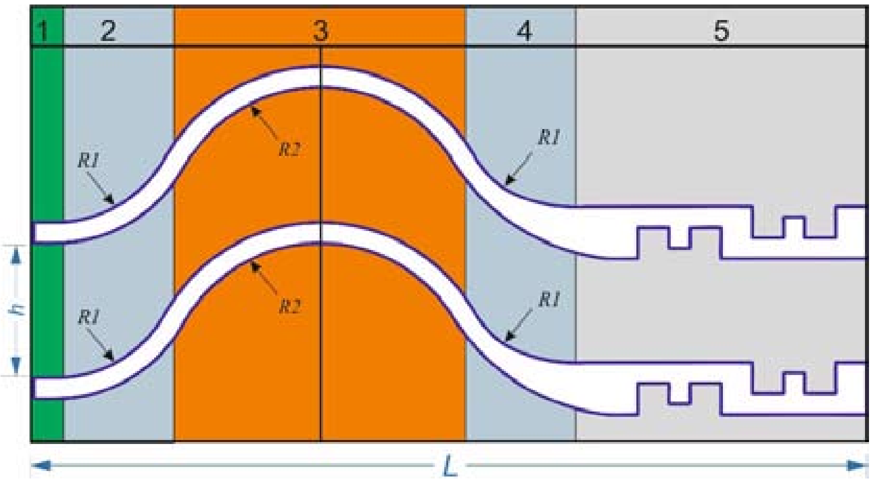

Fig. 1. Structure diagram of the separating profile with varying curvature radii and dimensions: $R1 = (0.05 \div 0.5)L$; $h = (0.5 \div 5.0)R1$; $R2 = (0.01 \div 1.0)L$:
1 — profile inlet; *2* — *R1* zone; *3* — *R2* zone; *4* — *R1* zone; *5* — droplet capture (demisting) zone

- calculation grid built of triangular segments with the area of $S = 30 \cdot 10^{-8}$ m²;
- environment parameters — normal conditions;
- gas density of $\rho_g = 1.225$ kg/m³;
- gas viscosity of $\mu_g = 1.79 \cdot 10^{-5}$ kg/(m·s);
- the channel wall material is aluminum with the roughness of 0.1 mm and density of $\rho_{al} = 2690$ kg/m³;
- minimal particle diameter of 3 μm;
- average particle diameter of 100 μm;
- maximum particle diameter of 150 μm;
- concentration of the liquid phase (H_2O) — 5, 10, 15, 20 %;
- velocity range — 5, 10, 15, 20 m/s.

Fig. 3 – 10 present the distribution of velocity (flow rate), kinetic energy of turbulence, static and dynamic pressure for the channel with the radii of 5, 10, 15, 20, 25 mm at U = 5…20 m/s. The calculation results indicate that the channel with the length of 80 mm and radius of 15 mm has the most efficient hydrodynamic characteristics.

Aerosol deposition in the separating profile has been calculated for the particle diameter of 1...3 μm, liquid phase concentration (H_2O) of 5, 10, 15, 20 % and the velocity range of 5, 10, 15, 20 m/s. At that, the problems of non-stationary conditions with the final step in time were solved with the Raising Rambler method for the particle trajectory to reach the deposition surface (the profile walls or the outlet cross section) in the calculation grid. The calculation assumed that the coincidence of the particle trajectories implied their combination (Table 1). The particle was considered to be captured if its trajectory coincided with the wall of the channel.

At the rate of 5...10 m/s, the deposition coefficient of the profile with the radius of 5 mm makes up 36.1...30.2 %. When the flow rate is increased up to 20 m/s, the liquid phase breaks away and the deposition coefficient decreases to 20.8 %. At the rates up to 5...10 m/s, the deposition coefficient of the profile with the radius of 10 mm makes up 91.9...90.4 %. When the flow rate is increased up to 20 m/s, the liquid phase breaks away and the deposition coefficient decreases to 51.9 %. At the rates up to 5...10 m/s, the deposition coefficient of the profile with the radius of 15 mm makes up 99.9...99.1 %. When the flow rate is increased up to 20 m/s, the liquid phase breaks away and the deposition coefficient decreases to 74.9%. At the rates up to 5...10 m/s, the deposition coefficient of the profile with the radius of 20 mm makes up 85.6...72.9 %. When the flow rate is increased up to 20 m/s, the liquid phase breaks away and the deposition coefficient decreases to 50.5%. At the rates up to 5...10 m/s, the deposition coefficient of the profile with the radius of 25 mm makes up 42.5...31.3 %. When the flow rate is increased up to 20 m/s, the liquid phase breaks away and the deposition coefficient decreases to 15.9 %.

Table 1. Calculation of the coefficient of deposition in the separating profile

R (mm)	*U* = 5 m/s				*U* = 10 m/s				*U* = 15 m/s				*U* = 20 m/s			
	5%	10%	15%	20%	5%	10%	15%	20%	5%	10%	15%	20%	5%	10%	15%	20%
5	35.7	34.7	35.8	36.1	31.3	31.2	31.4	30.2	25.9	24.8	25.7	26.4	20.8	20.6	20.4	20.2
10	91.6	91.4	91.3	91.9	94.8	92.8	91.3	90.4	70.9	69.4	68.2	68.3	51.9	50.3	50.5	49.4
15	99.9	99.9	99.9	99.9	99.6	99.3	99.4	99.1	82.3	82.4	83.5	84.9	74.9	73.5	74.1	73.8
20	84.3	85.1	85.6	85.5	82.0	78.9	74.4	72.9	61.3	61.6	60.8	60.3	50.5	50.4	49.7	48.4
25	42.5	42.1	41.9	41.2	32.0	32.5	31.3	31.4	22.7	22.4	21.8	21.4	15.4	15.1	15.9	14.6

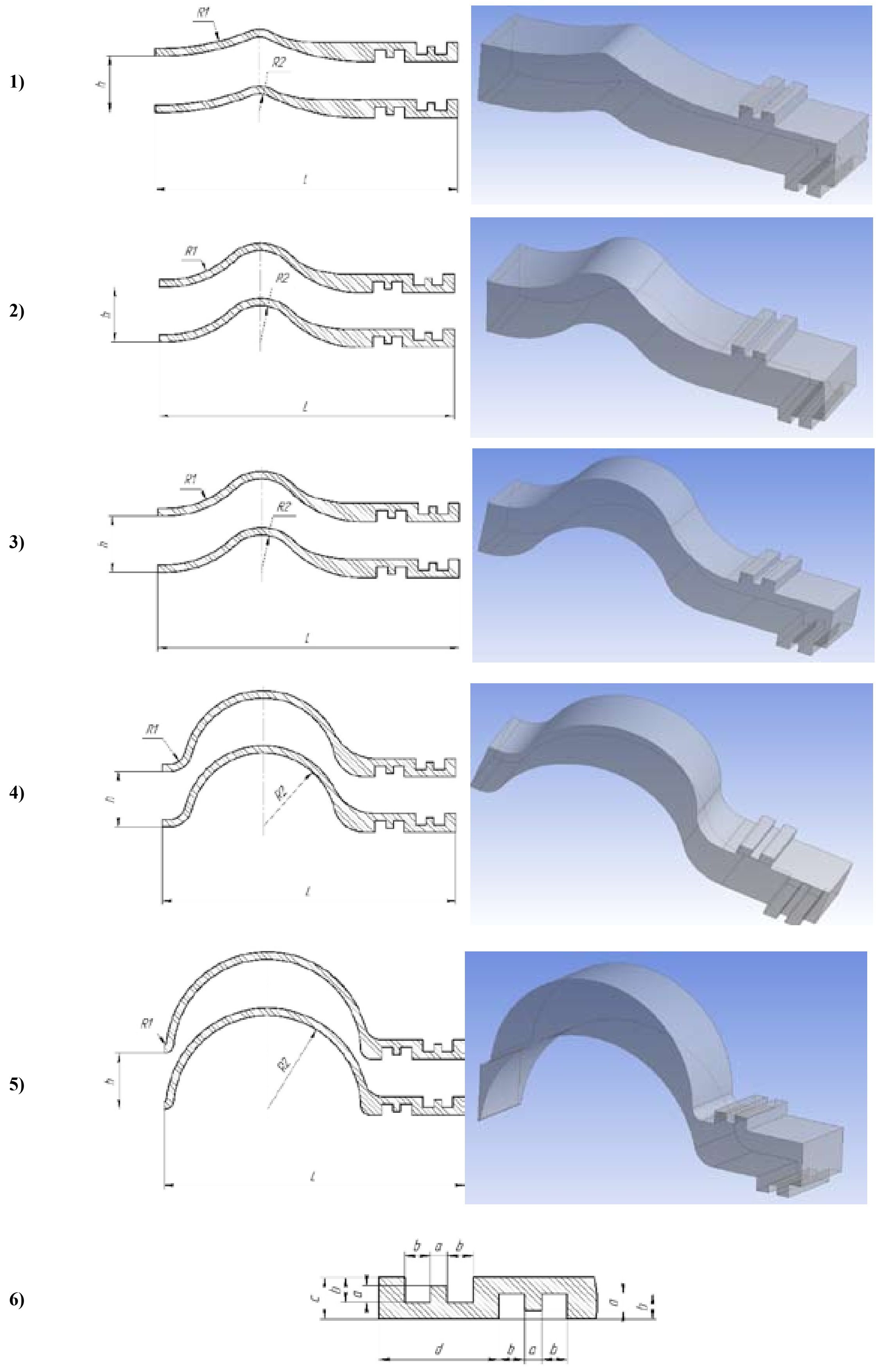

Fig. 2. Calculation grid of the three-dimensional operational geometry of the separating profile: 1) *R1* = 60 mm, *R2* = 5 mm, *h* = 15 mm, *L* = 80 mm; 2) *R1* = 25 mm, *R2* = 10 mm, *h* = 15 mm, *L* = 80 mm; 3) *R1* = 12 mm, *R2* = 15 mm, *h* = 15 mm, *L* = 80 mm; 4) *R1* = 4 mm, *R2* = 20 mm, *h* = 15 mm, *L* = 80 mm; 5) *R1* = 1 mm, *R2* = 25 mm, *h* = 15 mm, *L* = 80 mm; 6) *a* = 2 mm, *b* = 3 mm, *c* = 5 mm, *d* = 14 mm

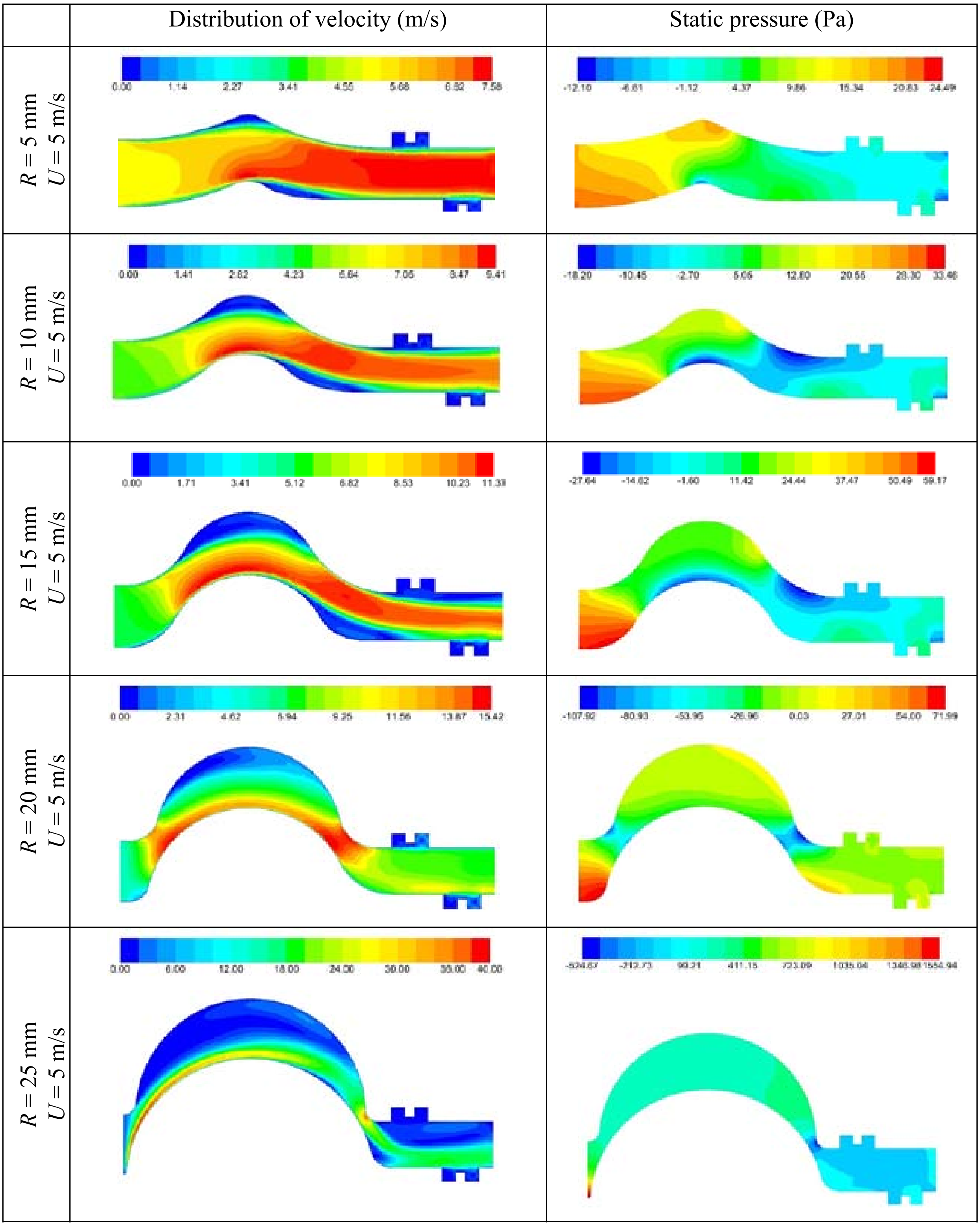

Fig. 3. Calculation of the distribution of velocity and static pressure for the channel radii of 5, 10, 15, 20, 25 mm at *U* = 5 m/s

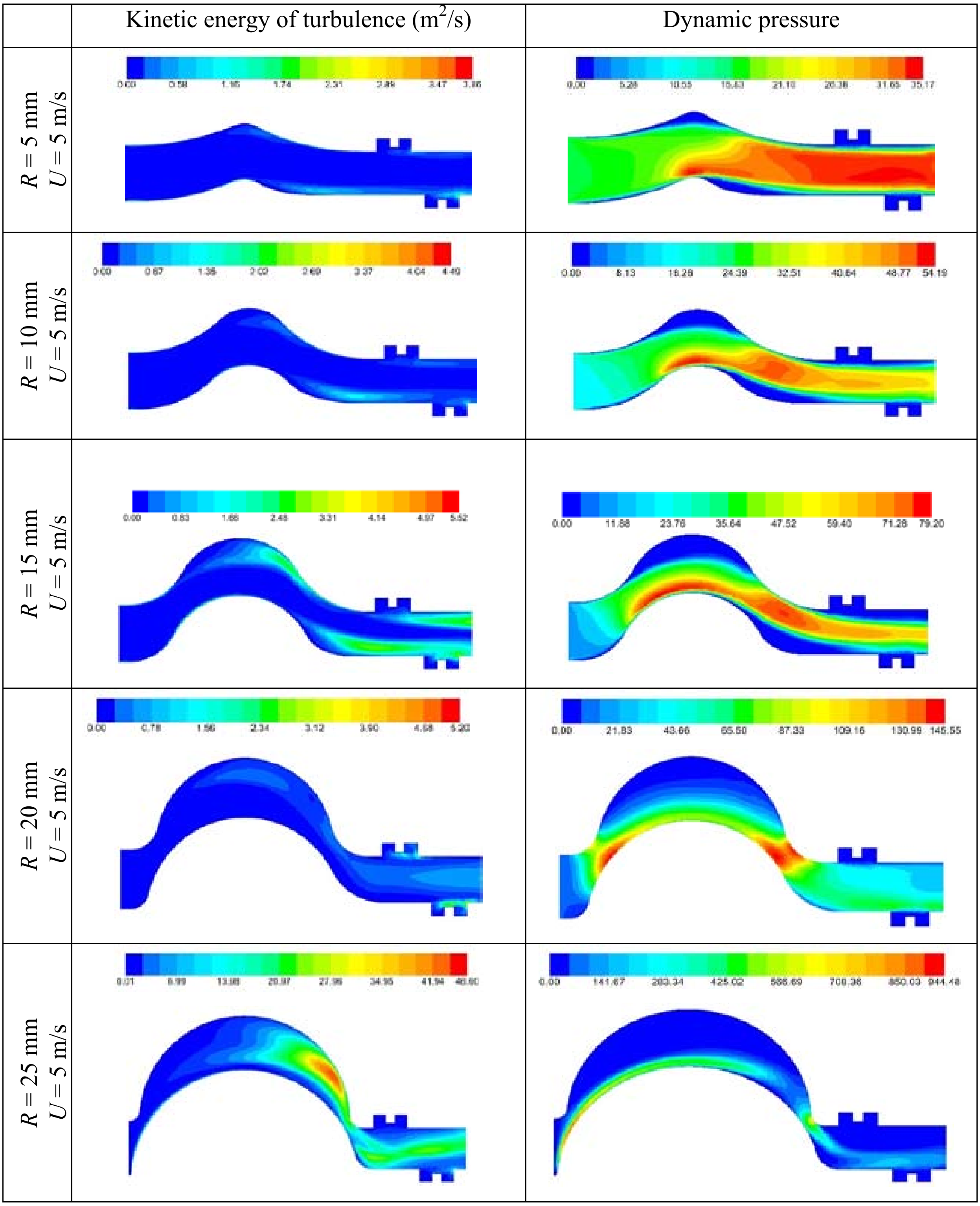

Fig. 4. Calculation of the distribution of kinetic energy of turbulence and dynamic pressure for the channel radii of 5, 10, 15, 20, 25 mm at *U* = 5 m/s

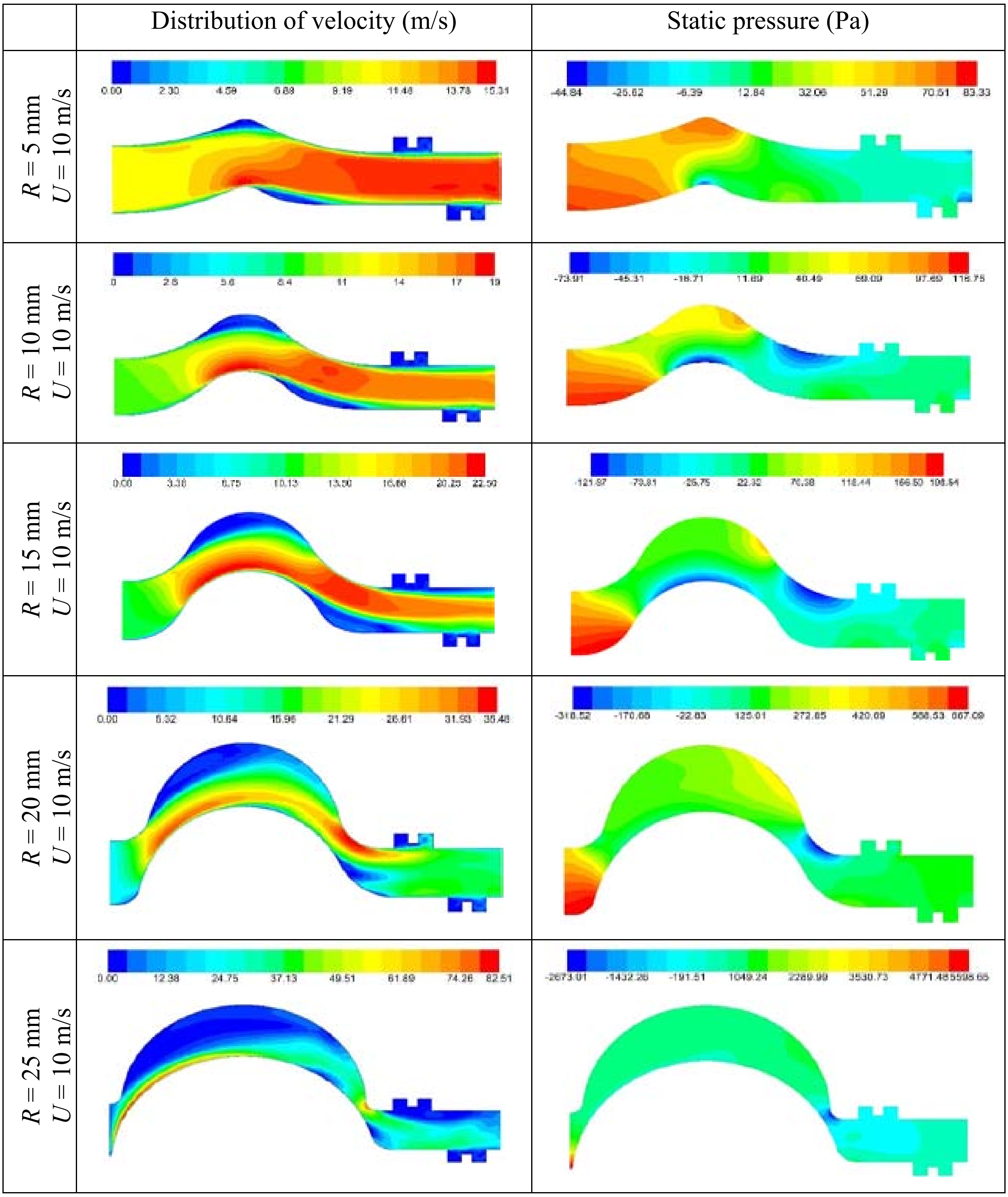

Fig. 5. Calculation of the distribution of velocity and static pressure for the channel radii of 5, 10, 15, 20, 25 mm at U = 10 m/s

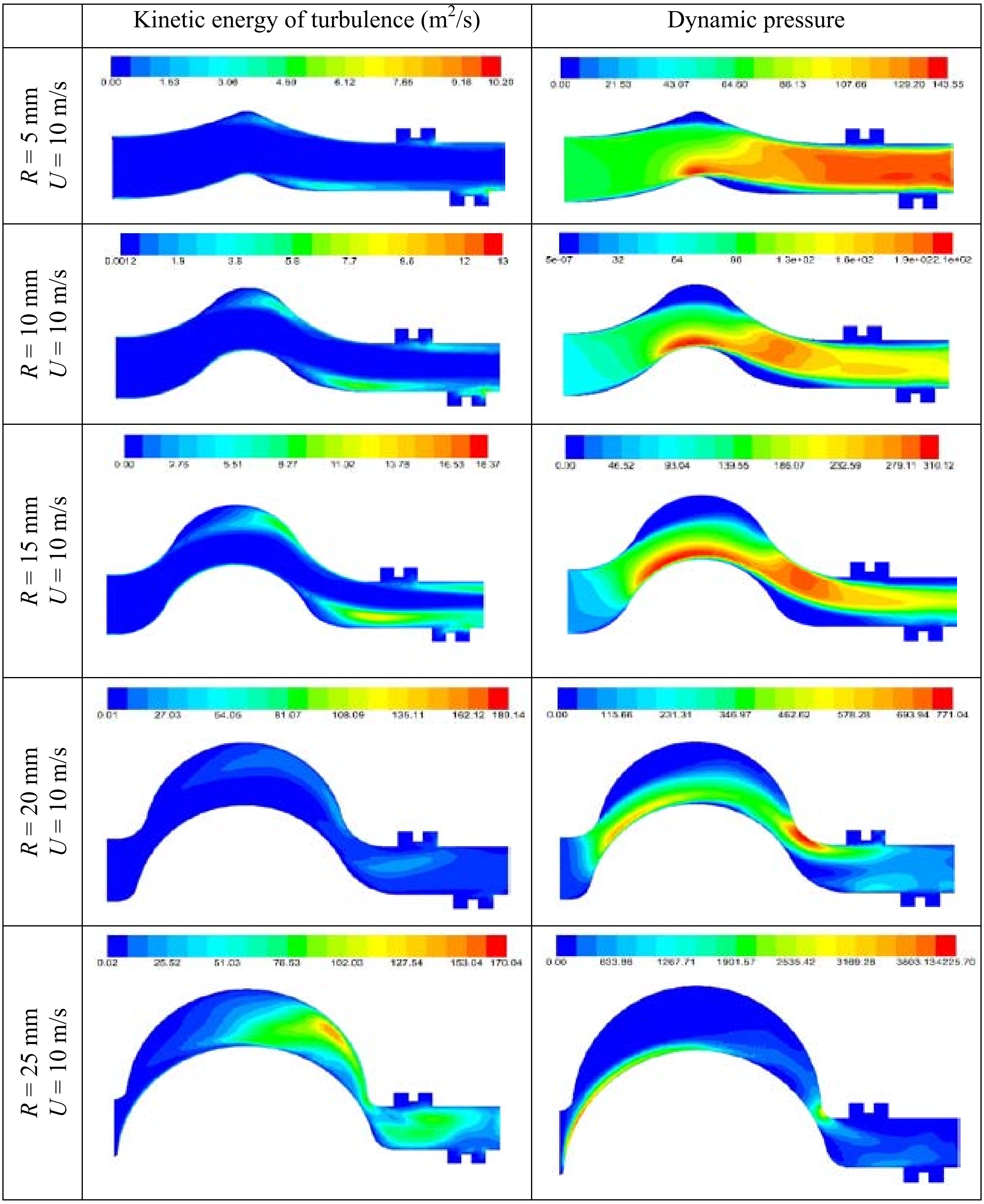

Fig. 6. Calculation of the distribution of kinetic energy of turbulence and dynamic pressure for the channel radii of 5, 10, 15, 20, 25 mm at $U = 10$ m/s

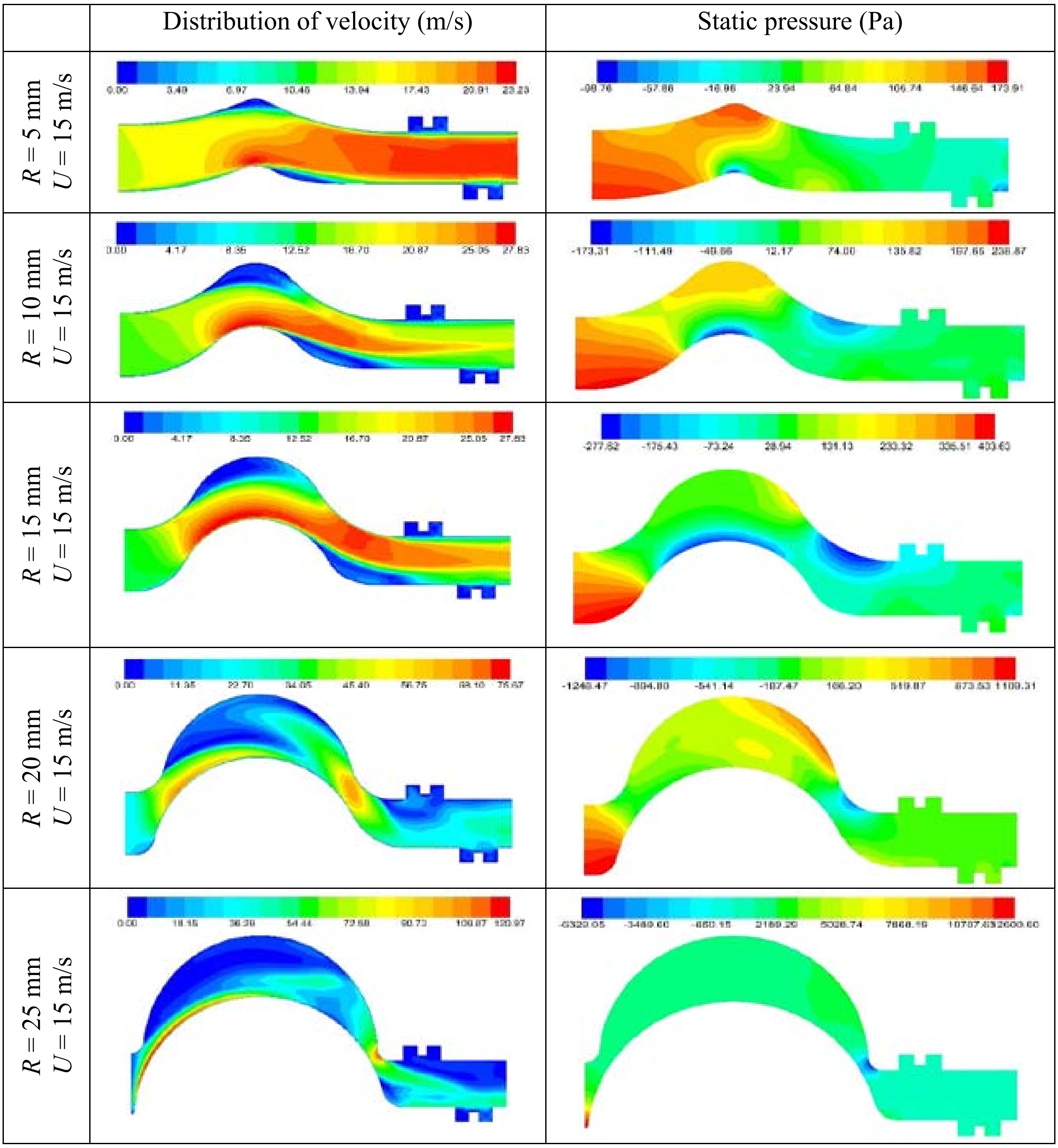

Fig. 7. Calculation of the distribution of velocity and static pressure for the channel radii of 5, 10, 15, 20, 25 mm at $U = 15$ m/s

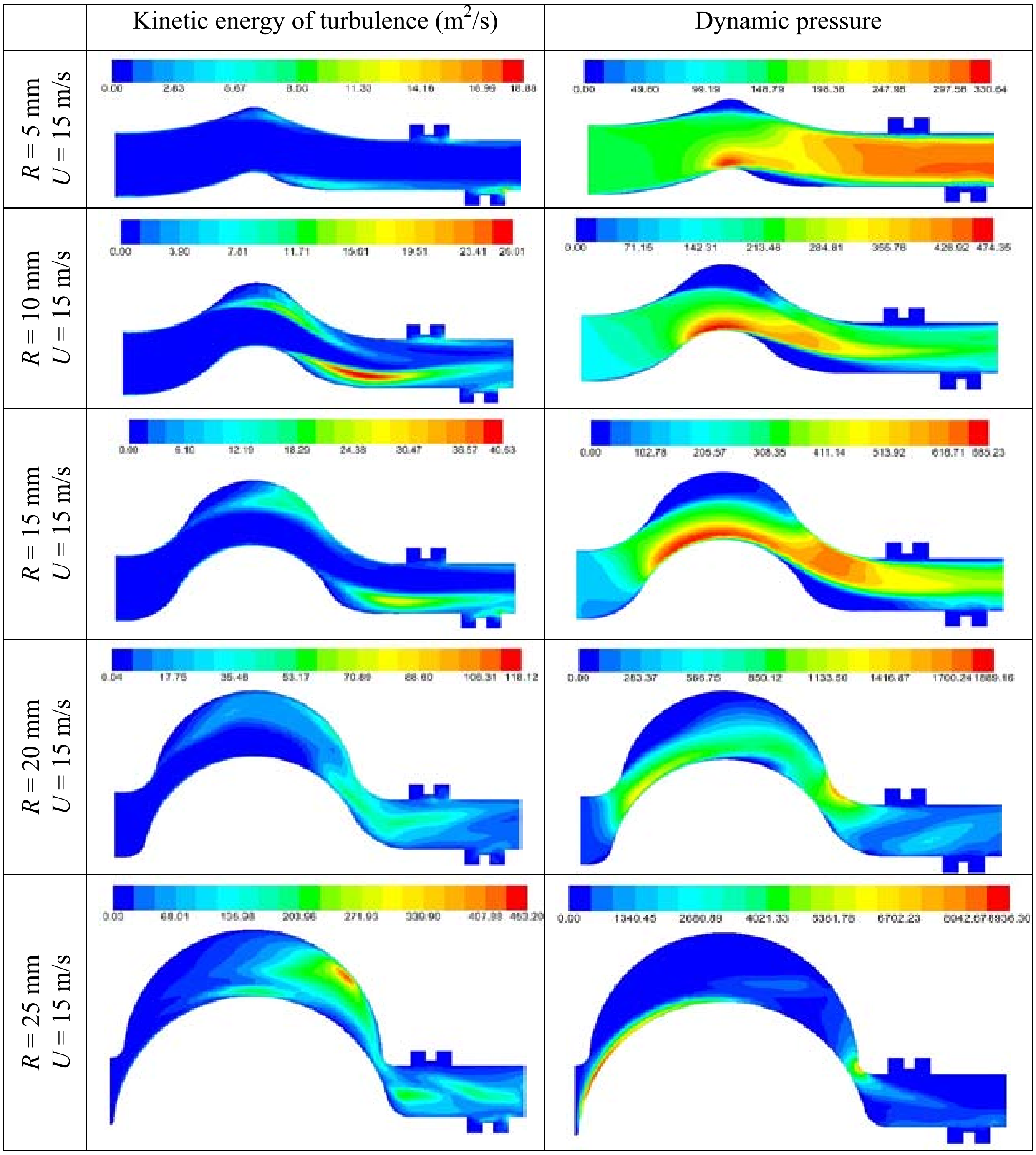

Fig. 8. Calculation of the distribution of kinetic energy of turbulence and dynamic pressure for the channel radii of 5, 10, 15, 20, 25 mm at U = 15 m/s

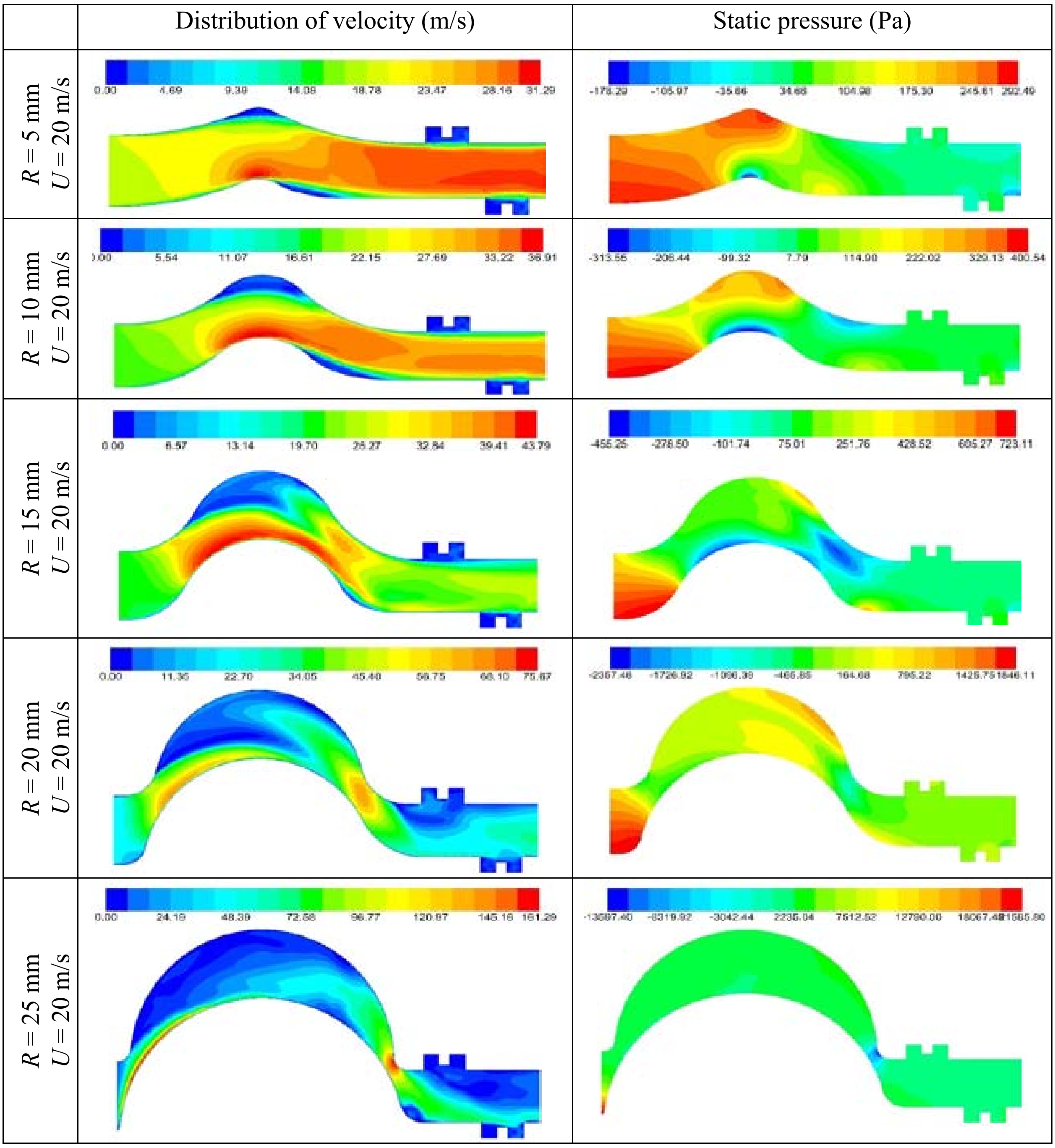

Fig. 9. Calculation of the distribution of velocity and static pressure for the channel radii of 5, 10, 15, 20, 25 mm at U = 20 m/s

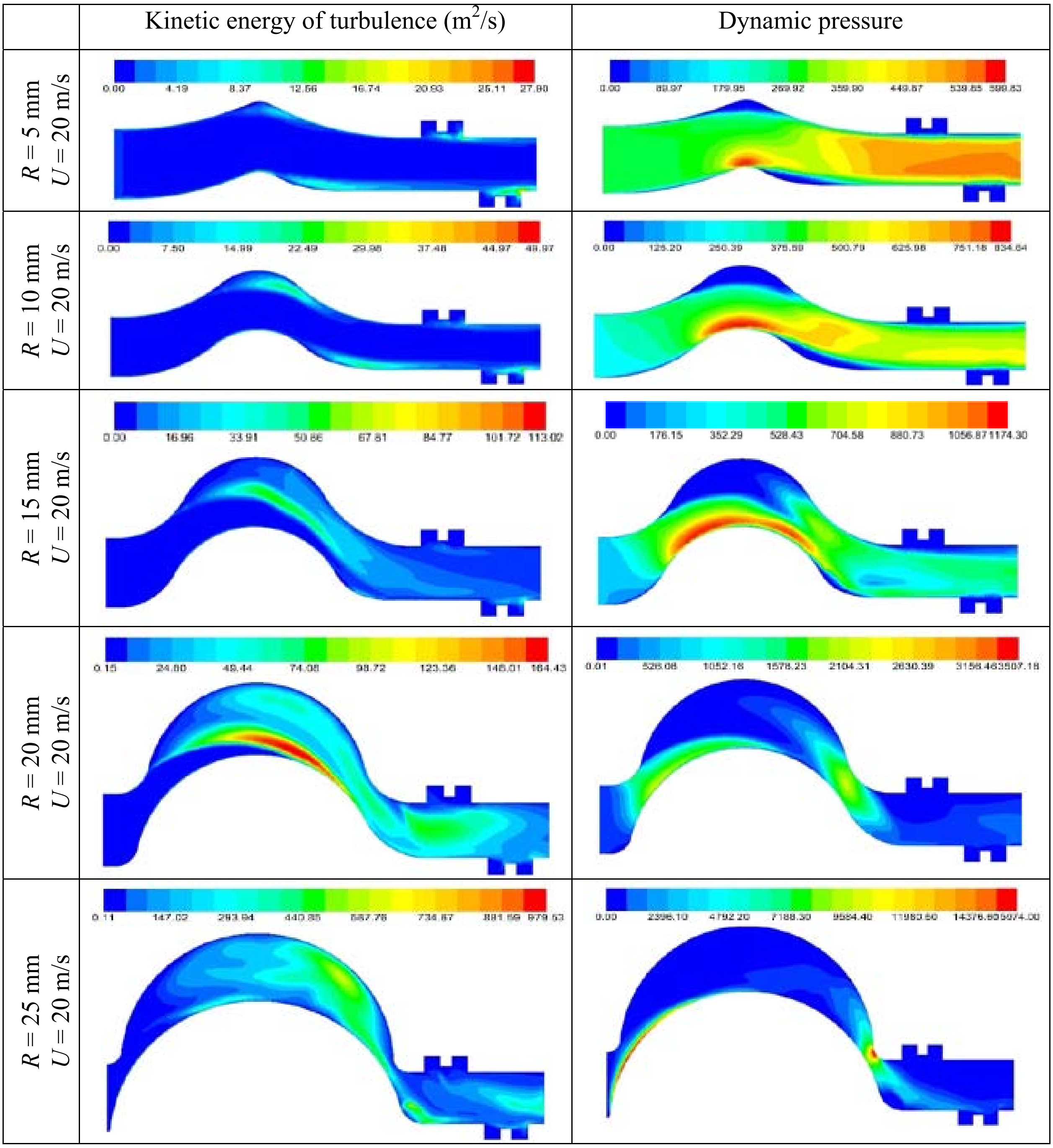

Fig. 10. Calculation of the distribution of kinetic energy of turbulence and dynamic pressure for the channel radii of 5, 10, 15, 20, 25 mm at U = 20 m/s

As a result, it has been established that the deposition channel with the radius of 15 mm and the velocity range of 1...10 m/s are the most efficient separation options.

Upon studying the most efficient radius of the separating profile and determining the working velocities in the channel, there has been developed a general scheme of ship air purification systems aimed at elimination of droplet moisture and created a three-dimensional model of the 1000×500×116 mm separator (Fig. 11). The model was taken as a basis for building a calculation grid (see Table 2 and Fig. 12) with the following parameters:

- hree-dimensional real-size geometry of 1000×500×116 mm;
- calculation grid built of triangular segments with the area of $S = 30 \cdot 10^{-8}$ m^2;
- environment parameters — normal conditions;
- gas density of $\rho_g = 1.225$ kg/m^3;
- gas viscosity of $\mu_g = 1.79 \cdot 10^{-5}$ kg/(m·s);
- the channel wall material is aluminum with the roughness of 0.1 mm and density of $\rho_{al} = 2690$ kg/m^3;
- minimal particle diameter d_{min} of 3 μm;
- average particle diameter d_{mid} of 100 μm;
- maximum particle diameter d_{max} of 150 μm;
- concentration of the liquid phase (H_2O) — 5, 10, 15, 20%;
- velocity range — 1, 2, 3, 4, 5, 6, 7, 8, 9, 10 m/s.

Air purification from droplet moisture that take place in ship systems involves moisture deposition on the surface of separating profiles and water drainage into a tray, without damage to the formed water film (secondary flooding of the flow). In the curved channel, droplets of water transported by the air flow are deposited under the action of inertial forces both on the convex (frontal) and concave part of the channel.

In ship air conditioners, the intake air velocity is within the range of 2...10 m/s, the concentration of droplet moisture reaches 30 g/kg, and the average weight diameter of droplets reaches 100–150 μm when water is being dispersed with mechanical nozzles and 200 μm when the film breaks away from the edges.

The droplet moisture deposition has been studied experimentally on a test stand in the form of an open-type aerodynamic tube. As a result, the maximum concentration of the liquid phase for this separating profile was established at the initial air velocity of $U = 1...10$ m/s.

The disperse air-water mixture was prepared in the mixing chamber with the help of mechanical and pneumatic nozzles. The dispersity was determined by means of the contact method, i.e. by applying droplets onto mirror plates with subsequent photographing. The separa-

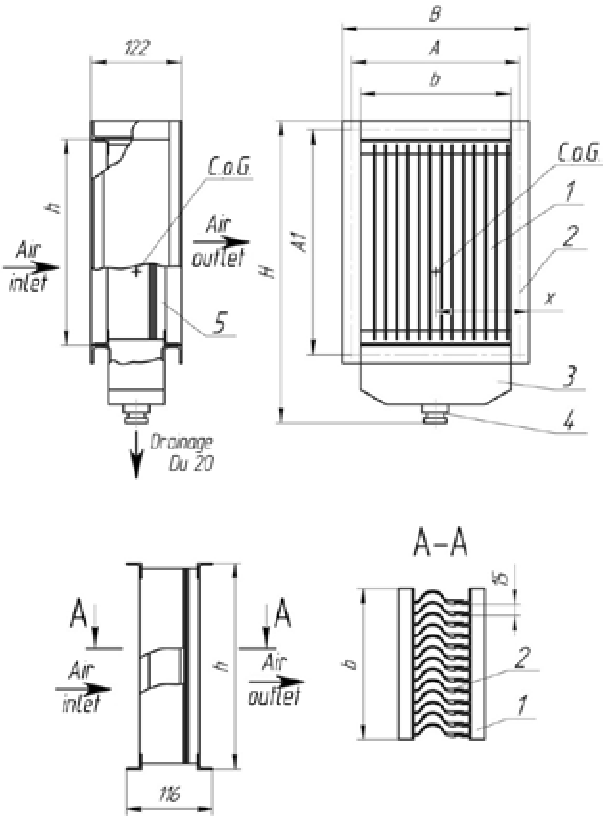

a)

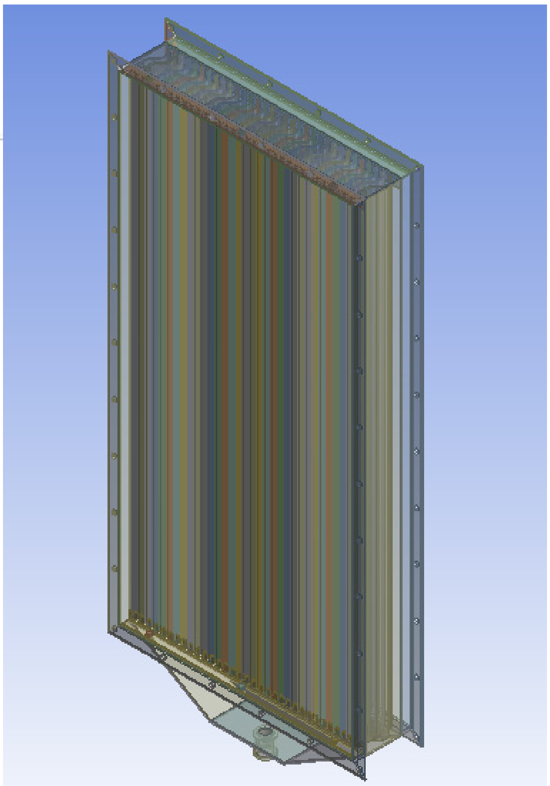

b)

Fig. 11. General scheme of ship systems for air purification from droplet moisture (*a*), three-dimensional model of the separator of 1000×500×116 mm (*b*):
1 — separating profile; *2* — fastening flange; *3* — drain tray; *4* — drain pipe; *5* — separating profile fastening; (for **A–A**: *1* — separating profile; *2* — separating profile fastening); *A*, *B A1*, *H*, *b*, *h* — equipment dimensions

Table 2. Calculation results for the deposition coefficient of the 1000×500×116 mm separator

U, m/s	Liquid phase concentration in the flow											
	5%			10%			15%			20%		
	d_{min}	d_{mid}	d_{max}	d_{min}	d_{mid}	d_{max}	d_{min}	d_{mid}	d_{max}	d_{min}	d_{mid}	d_{max}
1	90.1	99.9	100	85.9	99.9	100	83.9	99.9	100	82.8	99.9	100
2	90.3	99.9	100	85.6	99.9	100	83.6	99.9	100	82.2	99.9	100
3	90.6	99.9	100	85.2	99.9	100	83.3	99.9	100	81.9	99.9	100
4	90.0	99.9	100	85.4	99.9	100	83.2	99.9	100	81.6	99.9	100
5	90.4	99.9	100	85.1	99.9	100	83.1	99.9	100	81.2	99.9	100
6	90.1	99.9	100	84.5	99.9	100	82.7	99.9	100	80.8	99.9	100
7	90.2	99.9	100	84.1	99.9	100	82.3	99.9	100	80.4	99.9	100
8	89.9	99.9	100	83.9	99.9	100	81.9	99.9	100	80.2	99.9	100
9	89.4	99.9	100	83.6	99.9	100	81.5	99.9	100	79.8	99.9	100
10	89.1	99.9	100	83.1	99.9	100	81.1	99.9	100	79.1	99.9	100

GENERAL THREE-DIMENSIONAL MODEL 1000×500×116 MM — Velocity distribution in the channel (m/s)

isosymmetry — *side view* — *top view*

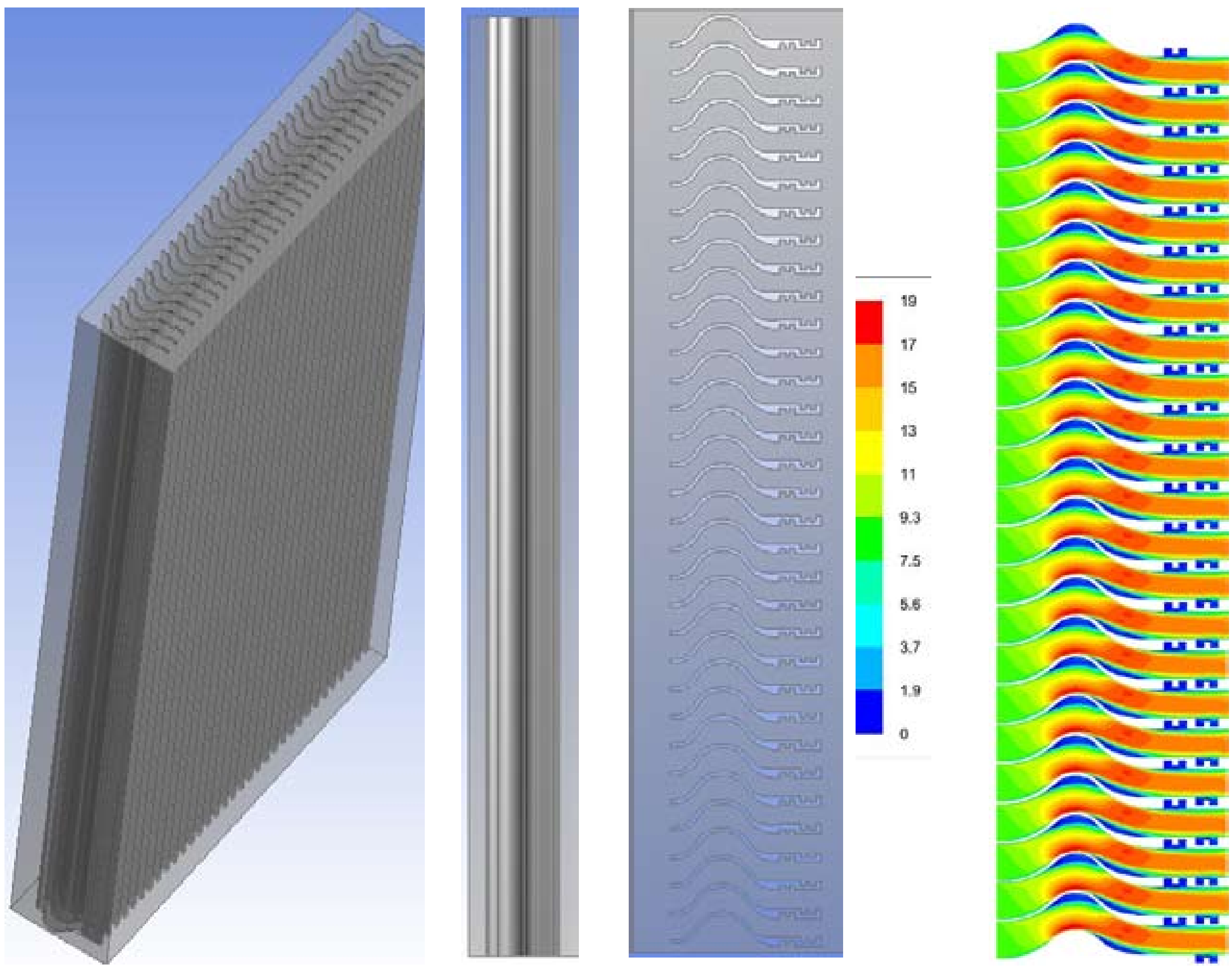

Fig. 12. Calculation grid and velocity calculation for the separator model of 1000×500×116 mm

tion ability was determined via three methods: material balance, contact method, and filtration with the help of analytical Petryanov filters.

The analysis has showed that droplets are deposited on the convex and concave parts of the profile in comparable amounts. As a result, two-side drain elements should be fitted into the separating profiles to prevent secondary flooding. A special feature of the profiles under development is a combination of a wave-shaped middle part with flat inlet and outlet parts. The profiles are assembled into curved channels with a number of successive converging and diffusing sections. The latter have breakaway zones with the reverse gas flow. There, the liquid film resulting from the deposition of droplets is subject to the impact of vortices which prevent the film movement with the main flow, contributing to its drainage under the action of gravity.

The vortex zones provide complete removal of the captured moisture from the smooth profile surface up to the velocity of 5 m/s. Above this velocity, some part of the moisture is removed from the vortex zones. That is why, special drain elements are provided to prevent secondary flooding of the flow in the flat section of the separating profile.

In air conditioning systems with surface heat exchangers, the main source of droplet moisture is the air cooler. The air flow breaks the condensate film away from the edges of the heat exchange surface, thus forming droplets. In the systems with contact devices, the processed air is saturated with moisture droplets in nozzle chambers, film machines, etc. The droplet size depends on the mode of spattering, the conditions of the water particles breakaway from the surface, and the essence of interaction of the particles with the air flow. Large droplets may be crushed under the impact of aerodynamic forces. Theoretical and experimental studies indicate that the disintegration of droplets is determined by the Weber number. When it exceeds 14, all the drops are disintegrated; the larger the Weber number is, the smaller the newly formed droplets are.

The conducted theoretical and experimental studies allowed for the development and approval of drawings for a lineup of ship systems for air purification from droplet moisture, as well as an enterprise standard for this lineup (Table 3–5).

Table 3. Experimental data for the deposition coefficient of the 1000×500×116 mm separator

U, m/s	Liquid phase concentration in the flow															
	5%	10%	15%	20%	25%	30%	35%	40%	45%	50%	55%	60%	65%	70%	75%	80%
1	99.9	99.9	99.9	99.9	99.9	94.9	91.4	90.6	81.1	79.2	75.0	71.9	67.8	61.7	55.4	53.1
2	99.9	99.9	99.9	99.9	99.9	94.1	91.9	91.3	81.8	78.4	75.1	71.2	66.4	62.9	55.4	51.9
3	99.9	99.9	99.9	99.9	99.9	95.9	91.0	91.6	81.9	79.3	74.8	70.9	67.7	63.8	54.2	50.4
4	99.9	99.9	99.9	99.9	99.9	95.4	91.1	91.2	81.3	78.9	74.1	69.0	68.5	62.3	55.2	51.1
5	99.9	99.9	99.9	99.9	99.9	95.1	91.9	90.2	80.3	79.6	73.0	68.8	69.4	61.3	54.2	51.9
6	99.9	99.9	99.9	99.9	99.9	90.1	84.8	89.9	78.9	71.9	68.9	61.9	63.2	54.1	49.9	45.9
7	99.9	99.9	99.9	99.9	99.9	82.9	82.5	82.2	74.1	69.2	62.1	57.1	53.9	49.4	44.1	39.9
8	99.9	99.9	99.9	99.9	99.9	80.3	79.3	74.9	70.7	64.3	57.8	52.0	47.3	41.6	37.8	32.9
9	99.9	99.9	99.9	99.9	99.9	78.2	77.1	71.2	66.4	59.9	51.2	45.7	41.2	36.7	32.5	26.9
10	99.9	99.9	99.9	99.9	99.9	83.9	75.9	69.9	61.9	54.9	46.9	41.8	35.9	31.9	28.2	24.9

Table 4. Classification of water separators

Types of water separators	General purpose
VVM	Main air/water separators for air conditioning and ventilation systems
VVM1	Main air/water separators for machine ventilation systems
VVK	Air/water separators of central air conditioners in air conditioning systems

Table 5. List of water separators by volumetric consumption

Designation	Volumetric air consumption, m3/h	Aerodynamic drag, Pa (mm of water column)	Working moisture saturation, g/kg of dry air	Separating property, % (marginal deviation — 1.0)
VVM 6.3	630 – 1600	40–250	20	100
VVM 10.0	1000–2500	55–315		
VVM 16.0	1600–4000	40–250		
VVM 25.0	2500–6300	40–250		
VVM 40.0	4000–10000	45–315		
VVM 63.0	6300–16000	40–250		
VVM1 100.0	10000–16000	60–155		
VVM1 160	16000–25000	65–150		
VVM1 250.0	25000–40000	92–235		
VVM1 400.0	30000–40000	100–160		
VVK 16.0	1600–4000	20–100		
VVK 25.0	2500–6300	25–125		
VVK 40.0	4000–10000	20–100		
VVK 63.0	6300–16000	20–155		

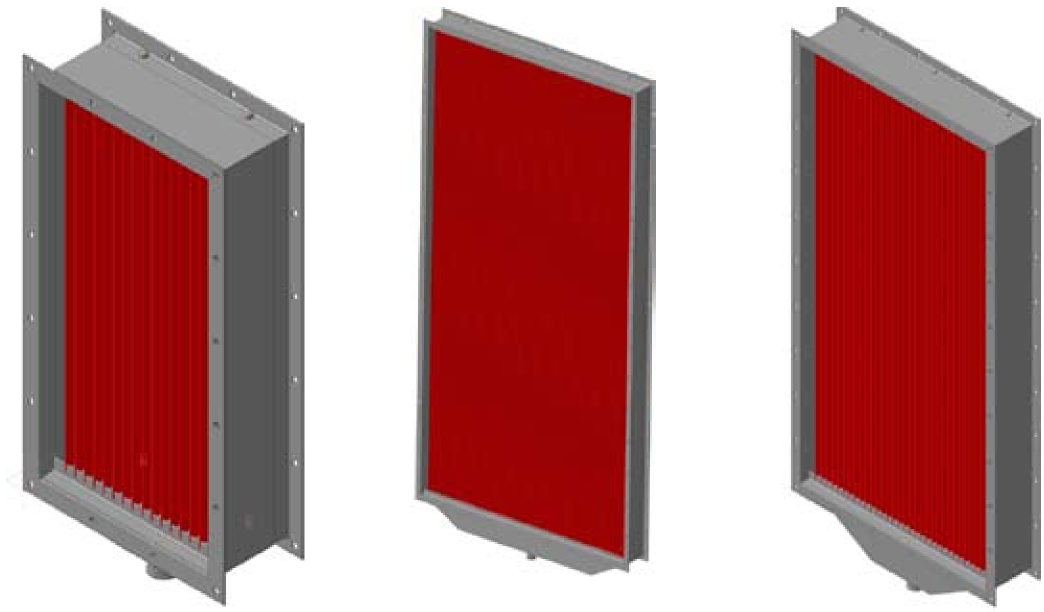

a) *b)* *c)*

Fig. 13. Three-dimensional exterior design of the ship system for air purification from droplet moisture:
a — 500×250×116 mm; *b* — 1000×500×116 mm; *c* — 2000×1000×116 mm

Fig. 13 demonstrates the typical design of a ship system for air purification from droplets moisture with a single-row package of separating profiles with the following dimensions: 500×250×116 mm, 1000×500×116 mm, 2000×1000×116 mm. They have been supplied with design documentation and working prototypes.

Tests of these water separators have showed that the capture coefficient is practically equal to 100% at the moisture saturation up to 50 g/kg and the intake air velocity up to 10 m/sec. At the velocity of 5 m/s, the aerodynamic drag makes up 50 N/m^2.

CONCLUSIONS. 1. Mathematical modeling of separation at the initial air velocity of 5, 10, 15, 20 m/s has been performed with the use of separation gradient aerosol technologies at different flow rates in separating profiles with the radii of 5, 10, 15, 20, 25 mm.

2. Distribution of velocity, static pressure, dynamic pressure, kinetic energy of turbulence and deposition coefficients has been calculated based on separation gradient aerosol technologies for the flow rates of 5, 10, 15, 20 m/s in separating profiles with the radii 5, 10, 15, 20, 25 mm. The coefficient of droplet moisture deposition was calculated for the flow rates of 5, 10, 15, 20 m/s in separating profiles with the radii 5, 10, 15, 20, 25 mm.

3. There have been developed design solutions for ship systems for air purification from droplet moisture for the air consumption ranging from 20 to 2000 m^3/h.

4. Drawings for a lineup of the ship air purification systems have been developed.

5. The enterprise standard for the lineup of the ship air purification systems has been developed.

Статью рекомендует в печать
д-р экон. наук, проф. *Н.И. Радченко*